water

MDPI

Article

Evaluating Carbon/Hydroxyapatite's Efficacy in Removing Heavy Metals from Groundwater

Qihui Yu [1,2,3,4], Hao Liu [1,2,3,5], Guocheng Lv [1,2,3], Xin Liu [1,2,3], Lijuan Wang [1,2,3], Lefu Mei [1,2,3] and Libing Liao [1,2,3,*]

[1] National Laboratory of Mineral Materials, School of Materials Science and Technology, China University of Geosciences, Beijing 100083, China; yuqihui2023@163.com (Q.Y.)
[2] Beijing Key Laboratory of Materials Utilization of Nonmetallic Minerals and Solid Wastes, China University of Geosciences, Beijing 100083, China
[3] Engineering Research Center of Ministry of Education for Geological Carbon Storage and Low Carbon Utilization of Resources, China University of Geosciences, Beijing 100083, China
[4] Development Research Center, General Technology Group Machine Tool Engineering Research Institute Co., Ltd., Beijing 100102, China
[5] School of Science, China University of Geosciences, Beijing 100083, China
* Correspondence: clayl@cugb.edu.cn

Abstract: Heavy metal pollution in groundwater and the environment poses a serious threat to ecosystems and human health. In particular, heavy metal ions, such as copper (Cu), zinc (Zn) and manganese (Mn), in the leachate of metal mine tailings ponds have attracted much attention due to their high toxicity and bioaccumulation. In order to solve the problem of heavy metal pollution in groundwater caused by leachate from tailings pond of a polymetallic mine, carbon/hydroxyapatite (CHAP) prepared from animal bones was used as the medium material to systematically study its removal effect on heavy metal ions in water under static and dynamic conditions. The static experiment results showed that CHAP had excellent adsorption properties for copper, zinc, manganese and mixed ions, and the adsorption capacities were up to 80 mg/g, 67.86 mg/g and 49.29 mg/g, respectively. Dynamic experiments further confirmed the application potential of CHAP as a Permeable Reactive Barrier (PRB) medium material, which can effectively remove heavy metal ions from flowing water, having a long service life. This study provides a theoretical basis and experimental reference for the in situ remediation of heavy metal-contaminated groundwater and shows the application prospect of CHAP in the field of environmental remediation.

Keywords: heavy metal pollution; PRB; carbon/hydroxyapatite; groundwater remediation; environmental pollution

check for updates

Academic Editors: Liting Hao and Qili Hu

Received: 5 February 2025
Revised: 28 February 2025
Accepted: 19 March 2025
Published: 21 March 2025

Citation: Yu, Q.; Liu, H.; Lv, G.; Liu, X.; Wang, L.; Mei, L.; Liao, L. Evaluating Carbon/Hydroxyapatite's Efficacy in Removing Heavy Metals from Groundwater. *Water* **2025**, *17*, 914. https://doi.org/10.3390/w17070914

Copyright: © 2025 by the authors. Licensee MDPI, Basel, Switzerland. This article is an open access article distributed under the terms and conditions of the Creative Commons Attribution (CC BY) license (https://creativecommons.org/licenses/by/4.0/).

1. Introduction

Heavy metal pollution is a global environmental problem with a wide range of sources, including industrial emissions [1,2], agricultural activities, mining [3] and smelting processes [4]. These heavy metals, such as lead (Pb) [5], copper (Cu) [6], zinc (Zn) [7] and manganese (Mn), not only pose a serious threat to the environment but also pose a potential risk to human health through the food chain [8,9]. Traditional heavy metal treatment technologies, such as chemical precipitation, ion exchange and membrane separation, have disadvantages such as a high cost, complex operation and possible secondary pollution [10–12]. Therefore, it is of great significance to develop new, efficient and economical heavy metal removal technology.

Permeable Reactive Barrier (PRB) technology, as a kind of in situ repair technology, has attracted wide attention due to its advantages such as high efficiency, economy and easy management [13,14]. PRB technology can remove heavy metals and other pollutants by setting reaction walls containing active materials in the underground water flow path and utilizing the chemical reaction between pollutants and active materials [15]. However, the efficiency and stability of PRB technology largely depend on the medium materials used [16].

As a new type of composite adsorption material, carbon/hydroxyapatite (CHAP) has attracted much attention due to its unique physical and chemical properties and high efficiency in heavy metal adsorption [17]. CHAP is composed of nano-hydroxyapatite and amorphous carbon, with a high specific surface area, rich functional groups and good pore structure, showing excellent heavy metal adsorption performance [18]. There is a small amount of research on the use of hydroxyapatite with or without carbon in PRB medium materials. For example, Kong et al. used bovine bone to make hydroxyapatite and carried out static and dynamic experiments on removing heavy metal copper from water. The static adsorption capacity of copper reached 25.7 mg/g. The dynamic experiment results showed that the hydroxyapatite synthesized from bovine bone had excellent hydraulic performance, no plugging occurred, and the pore volume PV value reached 450. The durability is stable, indicating that bovine hydroxyapatite is a high-quality adsorbent and can be used for the in situ remediation of copper-contaminated groundwater [19]. Fuller et al. investigated the binding of uranium to white bone char and bone powder apatite materials in the presence and absence of dissolved carbonate and also investigated granular white bone char recovered from PRBs. The results show that under groundwater conditions in many uranium-contaminated sites, uranium absorption by bone apatite may occur through surface complexation [20].

As an important solid waste, heavy metal tailings pollute water in many ways. The main feature is that the tailings have small particles, so they are more likely to have geochemical reactions with microorganisms and rainfall, resulting in the release of stable heavy metals in minerals into water and soil in the form of ions [21]. On the other hand, tailings not only contain a variety of heavy metal elements, such as arsenic, cadmium, lead and zinc, but also non-metallic pollutants, such as sulfur. For example, arsenic can leach into the environment through tailings stacking, rain and natural weathering [22]. The mineral structures in the tailings of lead and zinc are easily destroyed in the long-term natural weathering process, the sulfide is transformed into sulfate [23], and the heavy metals lead and zinc directly enter the surface water, groundwater and soil with the leaching of precipitation, causing great safety hazards [24]. Not only lead and zinc mines but also other heavy metal tailings ponds are affected by wind and rain, resulting in heavy metal infiltration, environmental pollution and ecological balance destruction. Multi-component heavy metals will cause more unpredictable damage to the environment, so exploring mixed heavy metal ions will have a positive effect on actual production and life.

In this study, animal bones were used as raw materials to prepare CHAP by optimizing heat treatment conditions. The adsorption performance of CHAP on Cu, Zn, Mn and their mixed ions under static conditions and the removal effect and service life evaluation of heavy metal ions under dynamic conditions were further studied. The maximum service life of CHAP for copper, zinc and manganese can reach 613.6, 458.65 and 204.14 PV, respectively. The mechanism of removing heavy metals using CHAP was briefly discussed. Through this study, the feasibility of CHAP as a medium material of PRB technology is verified, aiming at providing a theoretical basis and technical support for the treatment of heavy metal pollution.

2. Materials and Methods

2.1. Preparation of Experimental Materials

The experimental material used in this study is carbon/hydroxyapatite synthesized from bovine bone. The synthesis of carbon/hydroxyapatite includes pretreatment and calcination under a reducing atmosphere, the purpose of which is to remove the remaining impurities, such as fat and protein [25], and the purpose of calcination under a reducing atmosphere is to synthesize hydroxyapatite composites with high adsorption properties. The preprocessing steps include taking 5 g of bone powder evenly piled on a porcelain boat, placing it into a muffle furnace heated at 5 °C/min to a temperature of 300 °C and allowing for thermal insulation for 2 h. The pre-treated bone meal was taken out after natural cooling and then crushed and graded for subsequent experiment. By taking a small amount of the pile after pretreatment of the sample in the porcelain boat, under a nitrogen atmosphere in a tube furnace at 500 °C and a temperature increase of 5 °C/min for the heating temperature, with a holding time 2 h, the synthesis of CHAP occurred. This step is conducted in an air-isolated tube furnace, ensuring high purity and stability of the product. In this study, market-purchased bone char (BC) was used for comparison in the mixed static experiment. Please refer to Text S1 for the relevant introduction of bone char.

The distilled water used in this study was purchased from Beijing Jingji Ningyang Technology Co., Ltd. (Beijing, China), the copper ($Cu(NO_3)_2 \cdot 3H_2O$) was purchased from Shanghai Meirel Chemical Technology Co., Ltd. (Shanghai, China), the zinc ($Zn(NO_3)_2 \cdot 6H_2O$) was purchased from Shanghai Meirel Chemical Technology Co., Ltd., and the manganese ($Mn(NO_3)_2 \cdot 4H_2O$) was purchased from Shanghai Meirel Chemical Technology Co., Ltd.; the purity of the reagents was greater than 99%.

2.2. Characterization and Analysis Methods

The static and dynamic experimental results of CHAP and the heavy metals were mainly used to characterize the concentration of heavy metal ions, the phase and functional groups of the centrifugal precipitates. The X-ray diffraction spectra of the reaction precipitate were recorded using a Bruker D8 Advance diffractometer (XRD, Bruker D8 Discover, Bruker AXS GmbH, Karlsruhe, Baden-Württemberg, Germany), and the morphology of the precipitate was characterized by high-resolution field emission transmission electron microscopy (HRTEM, JEM-2100F, Kitaku, Japan). A Fourier transform infrared spectrometer (FT-IR, NICOLET iS20, Thermo Fisher Technology Co., Ltd., Waltham, MA, USA) and X-ray photoelectron spectroscopy (XPS, Escalab 250Xi, Thermo Fisher Scientific, USA) were used to characterize the changes in the functional groups before and after the reaction. The concentration of heavy metals was determined using an inductively coupled plasma spectrometer (ICP, Thermo scientific iCAP7609, Waltham, MA, USA).

In this study, Jade 6 was used for xrd analysis, Advange 5.9 was used for XPS analysis, and Origin2016 was used for drawing and fitting the results.

2.3. Experimental Method for Removal of Heavy Metals

The experimental methods include the static adsorption experiment and dynamic penetration experiment to evaluate the removal effect of CHAP on heavy metal ions in water.

2.3.1. Static Adsorption Experiment

Static adsorption experiments were carried out by mixing a certain amount of CHAP with a solution containing heavy metal ions at a set time and oscillating speed. After the reaction, the supernatant was separated via centrifugation, and the concentration change in heavy metal ions was analyzed using an inductively coupled plasma spectrometer (ICP)

so as to calculate the adsorption amount and removal rate of CHAP. The specific steps were weighing 0.04 g of the adsorbent sample and 20 mL of the heavy metal ion solution into a beaker and oscillating them in an oscillator at a speed of 200 r/min. By changing the concentration of the heavy metal solution and controlling the contact time between the sample and the heavy metal solution, the influence of the initial concentration and reaction time on the removal effect was explored. After the reaction, the mixture was centrifuged at a speed of 10,000 r/min for 5 min, we removed the supernatant to analyze the concentration of heavy metal ions as the equilibrium ion concentration *Ct* after the reaction, and we calculated the removal capacity. The formula is as follows:

$$Q = (C_0 - C_e)\, V/m$$

Among them, C_0 (mg/L) is the initial concentration of the heavy metal solution, C_t (mg/L) is the equilibrium concentration after the reaction, V (L) is the volume of the heavy metal solution, and m (g) is the mass of the sample. The centrifugal sediment underwent drying after recovery, related characterization and testing. The results of all batches of experiments are the average of the results of three parallel experiments.

In the static experiment to explore a single heavy metal, the dosage of CHAP was 0.04 g, and the initial concentrations of copper were set to 50, 100, 200, 300, 500, 1000, 1500 and 2000 g/L. The initial concentrations of zinc and manganese were set to 50, 100, 200, 300, 400, 600, 800 and 1000 mg/L, respectively, and 20 mL of contaminated liquid was collected. The CHAP and copper solution were placed into a centrifuge tube to react for 12 h. After the reaction, the supernatant was centrifuged, and the copper concentration was measured.

The adsorption times of copper and zinc were 0.5, 1, 2, 4, 8, 12, 16, 24 and 48 h. The 0.04 g sample was used to react with 20 mL of copper solution of 1000 mg/L and zinc solution of 500 mg/L in a centrifuge tube. The selected adsorption times for manganese were 0.5, 2, 4, 8, 16, 24 and 32 h, and the reaction time with 500 mg/L manganese solution was stopped after the specified time was reached. The supernatant was centrifuged to test the copper concentration, and the precipitate was retained for analysis and characterization.

2.3.2. Dynamic Penetration Experiment

The dynamic penetration experiment simulates the dynamic conditions in the actual water treatment process by filling CHAP in the experimental column and using a peristaltic pump to pass the heavy metal solution through the experimental column at a set flow rate. Samples were taken at different time intervals to analyze the concentration of heavy metal ions in the effluent, as well as to evaluate the removal capacity of CHAP and the service life of the test column.

First, 5 g of the carbon/hydroxyapatite samples with a particle size of 10~50 mesh were loaded into the experimental column with a length of 12 cm and an inner diameter of 22 mm, and the upper and lower layers were filled with quartz sand (particle size of 10 mesh and height of 3.5 cm). The peristaltic pump was used to pump the heavy metal solution from bottom to top to the placed experimental column to ensure that the mother liquor could fully contact the sample. The flow rate range of groundwater is usually wide, which can be determined according to terrain and hydrogeological parameters. In this study, the flow rate of peristaltic pump was set at 1.0035 mL/min, which is slightly higher than the average flow rate of groundwater. The life of the dynamic experimental column utilized under this condition will be lower than that of practical application, ensuring that CHAP has better use effect in practical application. Different initial concentrations are set according to the removal ability of CHAP for different heavy metal ions. The liquid flowing out of the test column was sampled at different time intervals to detect and analyze the concentration of heavy metal ions, and the removal ability of CHAP to pollutants and the

service life of the test column were evaluated. The experimental flow chart of this study is shown in Figure 1.

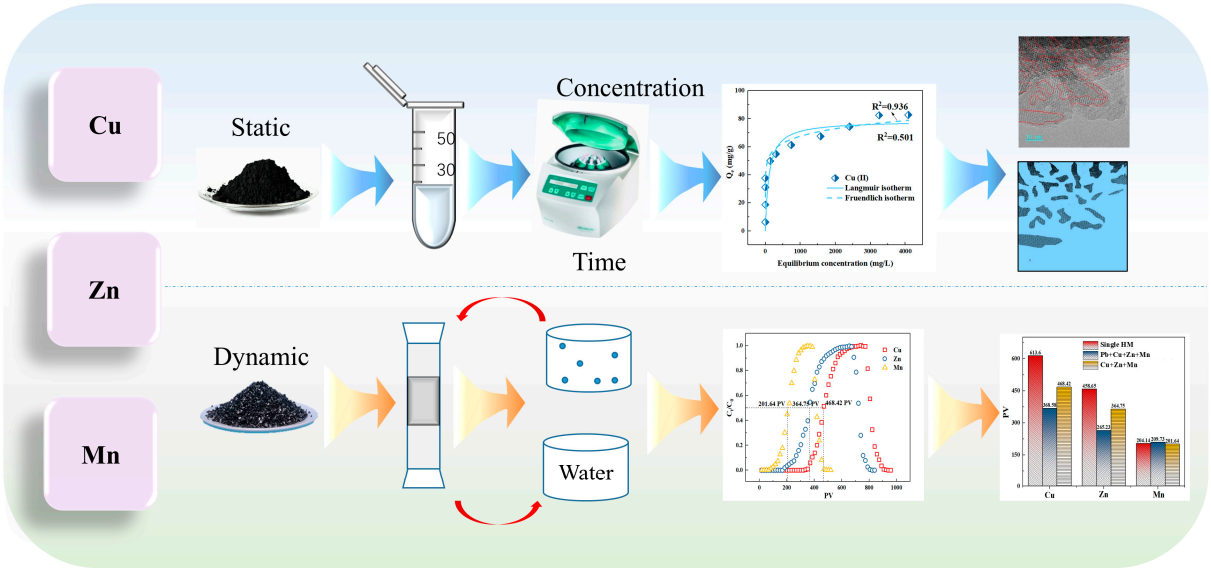


Figure 1. Research roadmap of this experiment.

3. Results and Discussion

3.1. Static Adsorption Experiment Results of Copper

Figure 2a shows the adsorption amount and removal rate of copper after the reaction of CHAP with a copper solution at different initial concentrations. The results show that when the initial concentration of copper is lower than 300 mg/L, the removal rate reaches more than 88.74%. When the initial concentration of copper is 2000 mg/L, the adsorption capacity reaches up to 80 mg/g. The copper adsorption capacity of CHAP is higher than that of other adsorbents [26–29]. Taking the equilibrium concentration as the X-axis and the adsorption capacity as the Y-axis, the Langmuir adsorption isotherm equation and Freundlich adsorption isotherm equation were used to fit the adsorption experimental data, and the results are shown in Figure 2b. The fitting results show that the adsorption of copper by CHAP was consistent with the Freundlich model, R^2 = 0.94. The detailed fitting parameters are shown in Table S1.

The kinetics of copper adsorption by CHAP was investigated. The results of copper adsorption by CHAP under different reaction times are shown in Figure 2c. Then, quasi-first-order and quasi-second-order kinetic fitting of the adsorption process is carried out. It can be seen from the figure that the process of copper adsorption by CHAP conforms to the quasi-second-order kinetic model, with R^2 = 0.985. The kinetic fitting parameters of CHAP adsorption of copper are shown in Table S2.

FT-IR spectra of CHAP and its reaction products with the copper solution are shown in Figure 2d. The FTIR spectra showed that the functional groups in CHAP did not change basically, indicating that there was no functional group complexation during the reaction with the copper solution. The C1s and Cu 2p XPS spectra of the products of CHAP reaction with the copper solution for 1 h and 24 h are shown in Figure 2e and f. The results showed that the valence states of copper and carbon in the products did not change at different reaction times, the content of copper and carbon changed slightly, and the binding energy moved slightly to the direction of higher binding energy.

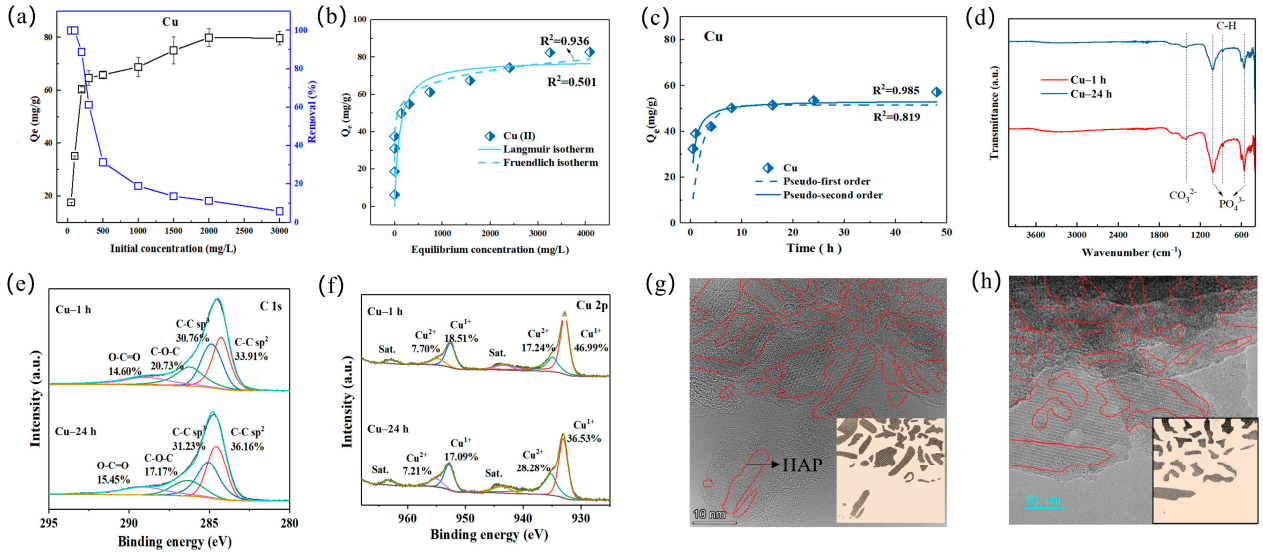


Figure 2. (**a**) Copper adsorption capacity and removal rate of CHAP under different initial concentrations; (**b**) Langmuir and Freundlich model fitting for CHAP adsorption of copper; (**c**) the amount of copper adsorption by CHAP under different reaction time conditions and quasi-first-order and quasi-second-order kinetic fitting of copper adsorption by CHAP; (**d**) the infrared spectrum of the products of CHAP reaction with the copper solution for 1 h and 24 h; (**e**) the C1s photoelectron spectra of the products of the CHAP reaction with the copper solution for 1 h and 24 h were obtained; (**f**) Cu 2p photoelectron spectra of the products of CHAP reaction with the copper solution for 1 h and 24 h; (**g**) the position relationship between hydroxyapatite and amorphous material in CHAP; TEM images of the reaction products of CHAP with the copper solution at different magnifications; (**h**) the position relationship between hydroxyapatite and amorphous material after the reaction of CHAP with the copper solution.

The binding energy of C-O and C=O functional groups decreased, and the binding energy of C-C and C=C functional groups increased when CHAP was used for lead removal, which was obviously different from that for copper removal [30,31]. Combined with the FT-IR spectral results, it is considered that the slight increase in XPS binding energy is a normal deviation of the test.

In addition, the initial morphology of CHAP and the morphology of the reaction products were analyzed using TEM. Figure 2g shows the lattice fringe of the hydroxyapatite phase in CHAP for measurement, which can clearly determine the distribution of hydroxyapatite and the amorphous matrix. In addition, the lattice fringe of the phase after the reaction of CHAP with copper was measured. The distribution of hydroxyapatite and the amorphous matrix is shown in Figure 2g,h, and the mapping element distribution of the sample after the reaction (Figure S1) showed that copper was uniformly distributed on the CHAP. According to the mapping scanning results, the sample contains 18.36% carbon, 31.66% oxygen, 29.85% calcium, 12.83% phosphorus and 7.3% copper. Combined with the above analysis results, it is speculated that copper ions are physically adsorbed on the CHAP surface, which is basically consistent with the results of adsorption of copper by hydroxyapatite in the references.

3.2. Static Adsorption Experiment Results of Zinc

The adsorption of zinc by CHAP was investigated using research methods similar to those in Section 3.1. The maximum zinc adsorption capacity of CHAP was 67.86 mg/g, and the fitting results showed that the adsorption of zinc by CHAP was consistent with the Langmuir model, with R^2 = 0.987. The results are shown in Figure 3a,b. The zinc adsorption capacity of CHAP is higher than that of other adsorbents [32,33].

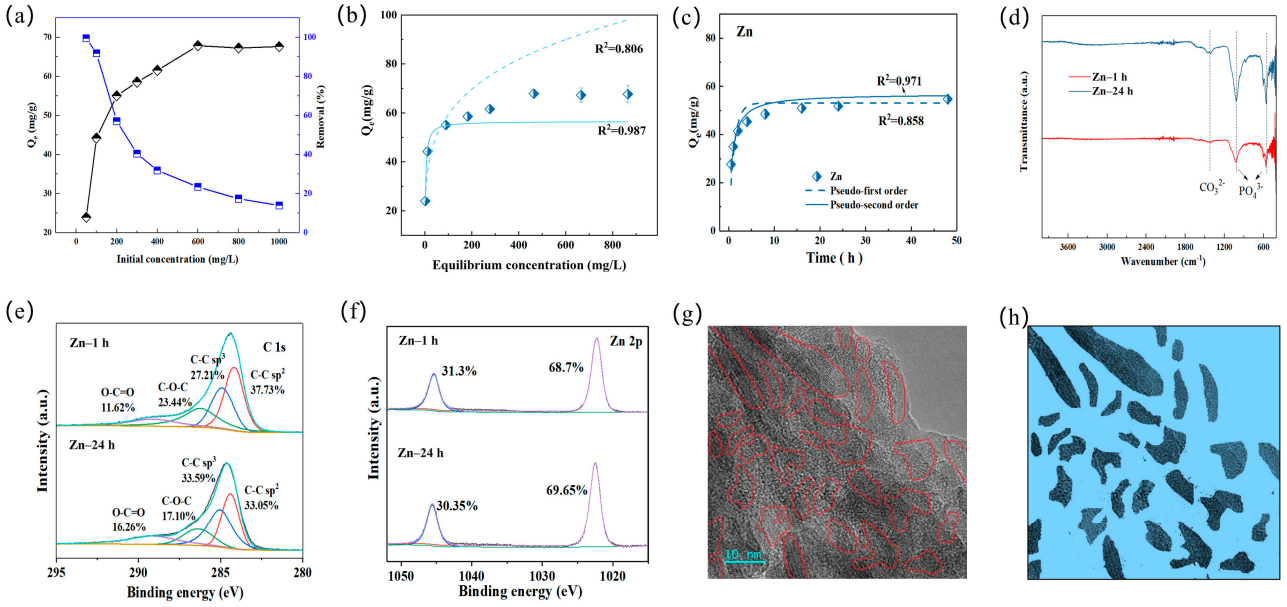


Figure 3. (**a**) Zinc adsorption capacity and removal rate of CHAP under different initial concentrations; (**b**) Langmuir and Freundlich model fitting for CHAP adsorption of zinc; (**c**) the amount of zinc adsorption by CHAP under different reaction time conditions and quasi-first-order and quasi-second-order kinetic fitting of zinc adsorption by CHAP; (**d**) the infrared spectrum of the products of the CHAP reaction with the zinc solution for 1 h and 24 h; (**e**) the C1s photoelectron spectra of the products of the CHAP reaction with the zinc solution for 1 h and 24 h were obtained; (**f**) Zn 2p photoelectron spectra of the products of CHAP reaction with zinc solution for 1 h and 24 h; (**g**,**h**) the position relationship between hydroxyapatite and amorphous material after the reaction of CHAP with the zinc solution.

Then, the adsorption kinetics of CHAP was studied. According to the equilibrium adsorption time of zinc removal by hydroxyapatite in the literature, the change in the zinc adsorption amount of CHAP with the reaction time is shown in Figure 3c. Quasi-first-order and quasi-second-order kinetic fitting of the process of zinc adsorption by CHAP was carried out, and the results are shown in Figure 3c. It can be seen from the figure that the process of zinc adsorption by CHAP conforms to the quasi-second-order kinetic model, with R^2 = 0.971.

FT-IR spectroscopy, XPS spectroscopy and TEM analysis of CHAP and the reaction products with zinc solution were performed. The results are shown in Figure 3d–h. The results showed that no new phase was formed. In addition, the mapping element analysis of CHAP was carried out, and the distribution is shown in Figure S2. The results showed that zinc was uniformly adsorped on CHAP. According to the morphology and element mapping analysis, the adsorption of zinc by CHAP belongs to physical adsorption.

3.3. Static Adsorption Experiment Results of Manganese

The adsorption of manganese by CHAP was investigated using research methods similar to those in Section 3.1. When the initial concentration is 1000 mg/L, the adsorption capacity is basically stable, and the maximum adsorption capacity is 49.29 mg/g (Figure 4a). The fitting results showed that the adsorption of manganese CHAP was more consistent with the Freundlich model, with R^2 = 0.971 (Figure 4b). The results showed that the adsorption of manganese by CHAP belonged to the combination of physical and chemical adsorption. The adsorption amount of manganese by CHAP is higher than that of other adsorbents [34].

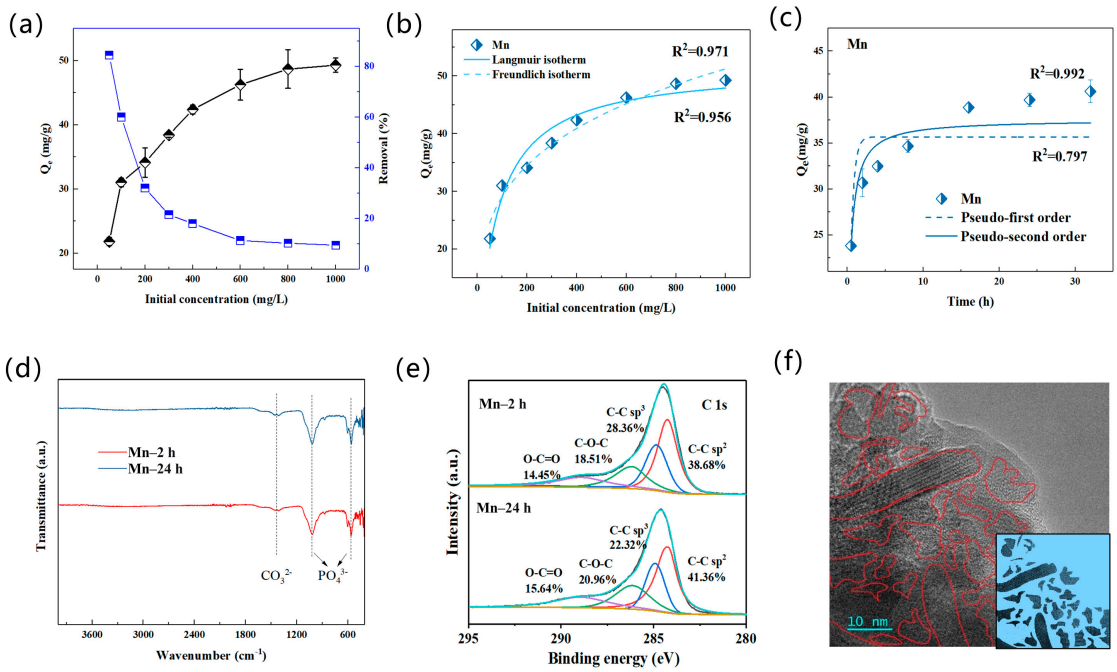


Figure 4. (**a**) Manganese adsorption capacity and removal rate of CHAP under different initial concentrations; (**b**) Langmuir and Freundlich model fitting for CHAP adsorption of manganese; (**c**) the amount of manganese adsorption by CHAP under different reaction time conditions and quasi-first-order and quasi-second-order kinetic fitting of zinc adsorption by CHAP; (**d**) the infrared spectrum of the products of the CHAP reaction with the manganese solution for 2 h and 24 h; (**e**) the C1s photoelectron spectra of the products of the CHAP reaction with the manganese solution for 1 h and 24 h were obtained; (**f**) the position relationship between hydroxyapatite and amorphous material after the reaction of CHAP with the manganese solution.

Kinetic experiments of manganese adsorption by CHAP were carried out. The change in the manganese adsorption capacity of CHAP with reaction time is shown in Figure 4c. Quasi-first-order and quasi-second-order kinetic fitting of the adsorption process was carried out, and the results are shown in Figure 4c. The process of CHAP adsorption of manganese was more consistent with the quasi-second-order kinetic model, R^2 = 0.992.

FT-IR spectroscopy, XPS spectroscopy and TEM analysis were performed on the CHAP and the reaction products with the manganese solution, and the results are shown in Figure 4d–f. The results showed that no new phase was formed. The position relationship between hydroxyapatite and the amorphous matrix was determined according to the lattice fringes observed after the reaction of CHAP with manganese, as shown in Figure 4f, which was similar to the adsorption of copper and zinc. The element distribution of the reaction product is shown in Figure S3, and manganese is uniformly distributed on the CHAP.

3.4. Static Mixed Adsorption Experiment Results

In this section, CHAP and BC were used to carry out static removal experiments on the mixed solution of copper, zinc and manganese to study the effect of the initial concentration of heavy metals on the removal effect. Due to the differences in the adsorption capacity of CHAP for the three heavy metal ions, the concentration ratio of copper, zinc and manganese is set at 5:2:2, and the specific initial concentration setting is shown in Table S3. The amount of adsorbent in each group was 0.04 g, the amount of mixed solution was 20 mL, and the reaction time was set to 8 h. CHAP and BC were, respectively, reacted with mixed heavy metal solutions numbered 1–8. After the reaction, the supernatant was centrifugated to test the concentration of each heavy metal so as to determine the adsorption amounts of CHAP and BC for different heavy metals.

A comparison of the adsorption amounts of copper ions removed from the mixed solution of three heavy metal ions by CHAP and BC is shown in Figure 5a. The adsorption capacity of copper ions removed by CHAP from the mixed solution is much higher than that of BC but lower than that of single copper ion removed by CHAP under this condition, indicating that zinc and manganese ions in the solution have competitive adsorption with copper ions. The removal of zinc ions from the mixed solution of three heavy metal ions by CHAP and BC is similar to the removal of copper ions, and the adsorption amount of zinc ions from the mixed solution by CHAP is only slightly higher than that of BC (Figure 5b). The removal of manganese ions from the mixed solution of three heavy metal ions by CHAP and BC was different, and the adsorption amount of manganese ions by BC was slightly higher than that by CHAP (Figure 5c). In the three heavy metal mixtures, the content of hydroxyapatite in BC is higher than that in CHAP (the carbon content of CHAP is higher), so the adsorption of manganese ions is higher than that of CHAP.

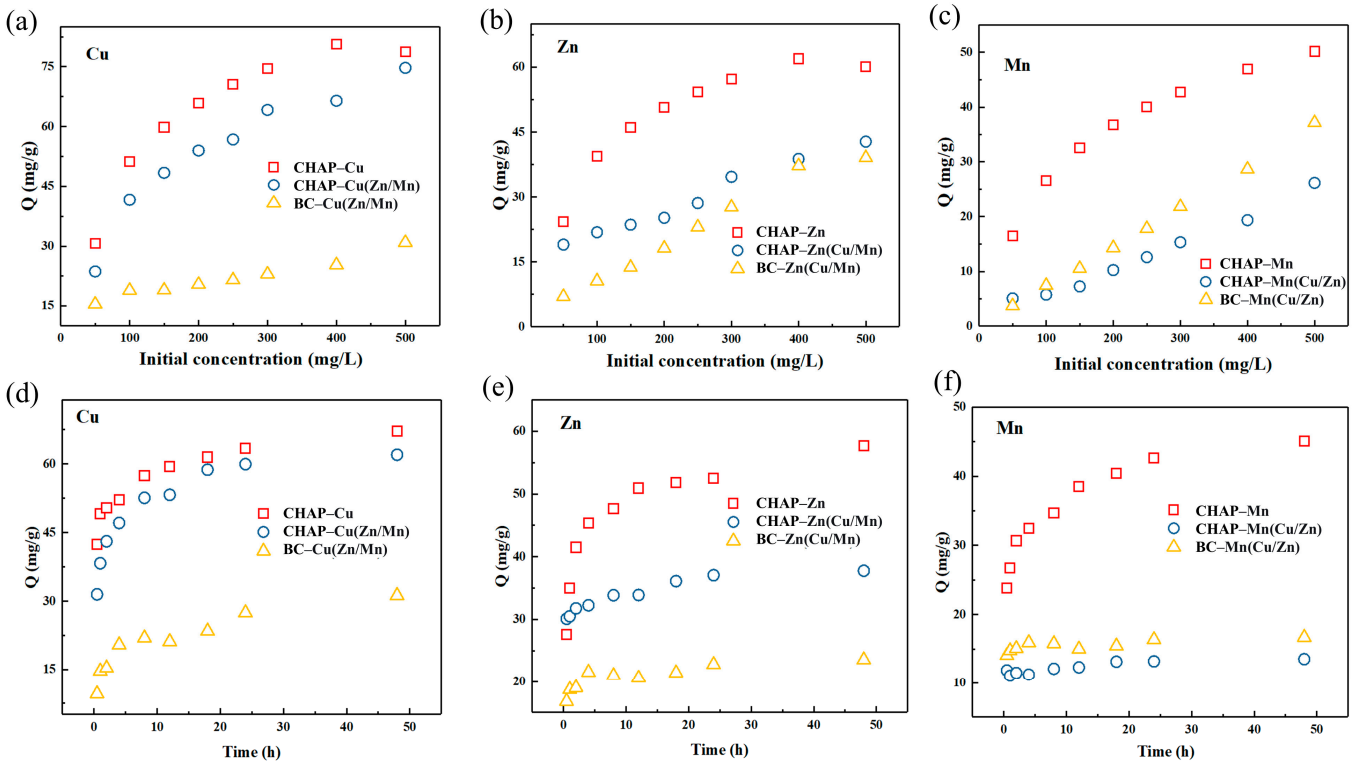


Figure 5. The adsorption capacity of heavy metal ions removed from mixed solution by CHAP and BC and the adsorption capacity of a single ion removed by CHAP: (**a**) copper, (**b**) zinc and (**c**) manganese; the adsorption capacity of copper (**d**), zinc (**e**) and manganese (**f**) ions after different reaction times of CHAP, BC and a mixed solution of metal ions and the adsorption capacity of single-ion removal.

Subsequently, experiments on the adsorption of copper, zinc and manganese ions in the mixed liquid of three metal ions by CHAP and BC under different reaction times were conducted, and the results are shown in Figure 5d–f. It can be seen that there is competitive adsorption among copper, zinc and manganese ions, and the presence of other metal ions has the least effect on the adsorption of copper ions by CHAP, followed by zinc ions, and the greatest effect on the adsorption of manganese ions. The adsorption of copper, zinc and manganese ions by CHAP was higher than that by BC. In summary, there is strong competitive adsorption between copper, zinc and manganese ions.

3.5. Dynamic Penetration Test Results

The dynamic removal curve of 10 mg/L copper ions by CHAP is shown in Figure 6a. The service life of the CHAP medium is 613.60 PV, the saturation life when it reaches fullness is 823.30 PV, and the corresponding running time is 49 days.

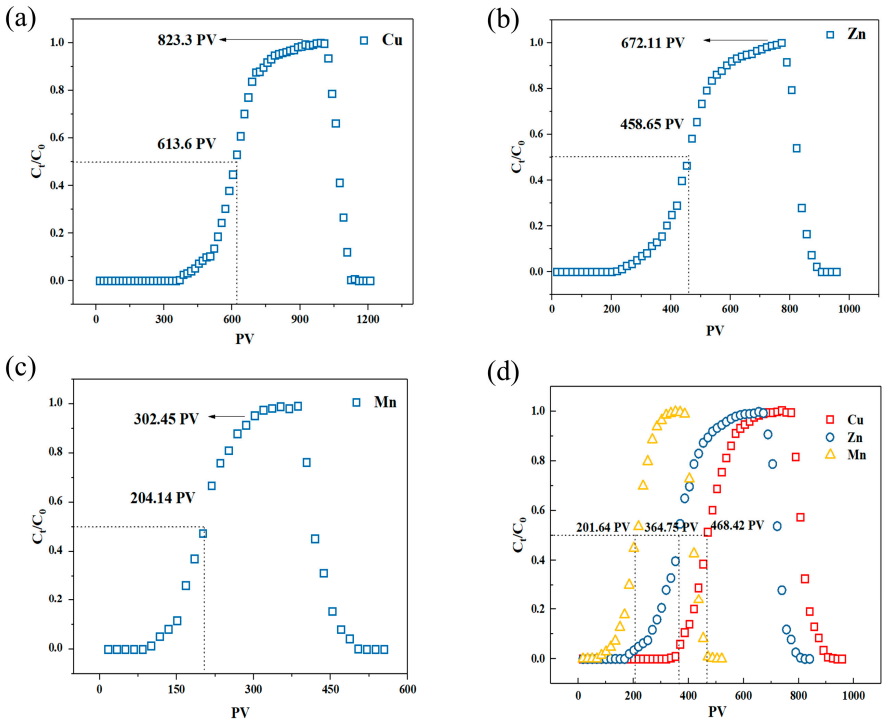


Figure 6. (**a**) Penetration curve of dynamic removal of copper ions by CHAP; (**b**) penetration curve of dynamic removal of zinc ions by CHAP; (**c**) penetration curve of dynamic removal of manganese ions by CHAP; (**d**) penetration curves of metal ions in copper, zinc and manganese mixed-ion solutions dynamically removed by CHAP.

The dynamic removal curve of 10 mg/L zinc ions by CHAP is shown in Figure 6b. The service life of the CHAP test column is 458.65 PV, the saturation life when reaching the saturation point is 672.11 PV, and the corresponding running time is 38 days.

The dynamic manganese removal curve of CHAP is shown in Figure 6c. The service life of CHAP test column is 204.14 PV and 302.45 PV when the saturation point is reached. The corresponding running time is 18 days.

As time goes by, the concentration of heavy metals in the effluent increases gradually until the saturation point is reached. The penetration curves of CHAP for Cu, Zn and Mn ions show that its service life is much longer than that of traditional materials, showing excellent long-term stability and removal efficiency.

A mixture of copper, zinc and manganese with a certain concentration was prepared as the simulated pollution solution (the initial concentration of copper was 10 mg/L, the initial concentration of zinc was 10 mg/L, and the initial concentration of manganese was 5 mg/L). The results of the mixed dynamic experiment (Figure 6d) show that in the solution for the combined removal of heavy metals containing copper, zinc and manganese, the saturation lifetimes of CHAP are 621.70, 529.94 and 285.65 PV, respectively. Due to the competitive adsorption among copper, zinc and manganese ions, when the three ions coexist, the service life and saturation lifetime are shortened. However, the impact is more significant on copper and zinc ions, while the impact on manganese ions is not obvious, which is not entirely consistent with the results of the static experiment. The competitive adsorption between metal ions has little effect on manganese ions, which have a small

adsorption capacity. The removal mechanism of Cu, Zn and Mn ions by CHAP under dynamic conditions needs further study.

4. Conclusions

In this study, carbon/hydroxyapatite composites (CHAP) were successfully prepared from animal bones, and their efficiency in removing heavy metal ions from water under static and dynamic conditions was comprehensively evaluated for the first time. CHAP showed a very high removal efficiency in static adsorption experiments, and the adsorption capacity of copper, zinc and manganese reached 80 mg/g, 67.86 mg/g and 49.29 mg/g, respectively, which was significantly higher than other adsorption materials in the existing literature. The dynamic experimental results further confirm the potential application value of CHAP as a permeation reaction grating medium. The service life of CHAP is up to 613.6 PV, and the saturation life is up to 823.3 PV. The excellent performance of CHAP under laboratory conditions provides a solid foundation and sufficient theoretical basis for its application in the actual environment. However, in order to ensure the effectiveness and stability of CHAP under different hydrogeological conditions, future research should focus on the interaction between ions under dynamic conditions, field tests and long-term monitoring. At the same time, considering the complex water chemical conditions that may be encountered in practical applications, further research on the removal effect of CHAP on other environmental pollutants and its potential environmental impact will help expand its application in the field of environmental remediation.

Supplementary Materials: The following supporting information can be downloaded at: https://www.mdpi.com/article/10.3390/w17070914/s1, Text S1. Composition and related characterization of bone char: Table S1. Fitting parameters of Langmuir and Freundlich models for copper adsorption by CHAP. Table S2. Quasi-first-order and quasi-second-order kinetic fitting parameters of copper adsorption by CHAP. Table S3. Concentration settings of three heavy metal mixtures. Figure S1. Element mapping of the reaction products of CHAP and copper solution. Figure S2. Element mapping of the reaction products of CHAP and zinc solution. Figure S3. Mapping of the reaction products of CHAP and manganese solution.

Author Contributions: Q.Y.: Methodology, Software, Investigation, Formal analysis, and Writing—original draft. H.L.: Resources, Formal analysis, and Writing—reviewing and editing. G.L.: Methodology. X.L.: Methodology. L.W.: Methodology. L.M.: Methodology. L.L.: Conceptualization, Funding acquisition, Resources, Supervision, and Methodology. All authors have read and agreed to the published version of the manuscript.

Funding: This work is financially supported by the National Natural Science Foundation of China (41831288).

Data Availability Statement: The original contributions presented in this study are included within the article/Supplementary Materials. Further inquiries can be directed to the corresponding author(s).

Conflicts of Interest: Author Qihui Yu was employed by the company Development Research Center, General Technology Group Machine Tool Engineering Research Institute Co., Ltd. The remaining authors declare that the research was conducted in the absence of any commercial or financial relationships that could be construed as a potential conflict of interest.

References

1. Yu, G.; Chen, F.; Zhang, H.; Wang, Z. Pollution and health risk assessment of heavy metals in soils of Guizhou, China. *Ecosyst. Health Sustain.* **2021**, *7*, 1859948. [CrossRef]
2. Sheremeti-Kabashi, F.; Kutllovci, F.; Mangjolli, B.; Hasani, A. Investigation of heavy metal concentrations in the Kelmend tailings landfill and ecological assessment of pollution. *Min. Miner. Depos.* **2024**, *18*, 110–118. [CrossRef]

3. Vesković, J.; Onjia, A. Environmental Implications of the Soil-to-Groundwater Migration of Heavy Metals in Mining Area Hotspots. *Metals* **2024**, *14*, 719. [CrossRef]
4. Xiao, R.; Guo, D.; Ali, A.; Mi, S.; Liu, T.; Ren, C.; Li, R.; Zhang, Z. Accumulation, ecological-health risks assessment, and source apportionment of heavy metals in paddy soils: A case study in Hanzhong, Shaanxi, China. *Environ. Pollut.* **2019**, *248*, 349–357. [CrossRef]
5. Xue, Y.; Teng, W.; Chen, Y.; Ma, Q.; Chen, X.; Sun, Y.; Fan, J.; Qiu, Y.; Fu, R. Amorphous Mn-La oxides immobilized on carbon sphere for efficient removal of As(V), Cd(II), and Pb(II): Co-adsorption and roles of Mn species. *Chem. Eng. J.* **2022**, *429*, 132262. [CrossRef]
6. Xiao, J.; Hu, R.; Chen, G. Micro-nano-engineered nitrogenous bone biochar developed with a ball-milling technique for high-efficiency removal of aquatic Cd(II), Cu(II) and Pb(II). *J. Hazard. Mater.* **2020**, *387*, 121980. [CrossRef]
7. Betts, A.R.; Chen, N.; Hamilton, J.G.; Peak, D. Rates and mechanisms of Zn^{2+} adsorption on a meat and bonemeal biochar. *Environ. Sci. Technol.* **2013**, *47*, 14350–14357. [CrossRef]
8. Rysbekov, K.; Yinli, B.; Demeuov, S.; Mukanova, G.; Zhakypbek, Y. Assessment of soil polution by heavy metals in the area of open mining works. *Vestn. KazNRTU* **2021**, *143*, 14–25. [CrossRef]
9. Aluwong, K.C.; Hashim, M.H.M.; Ismail, S.; Shehu, S.A. Physico-chemical assessment of surface water from mining activities in Maiganga coal mine, Gombe state, Nigeria. *Min. Miner. Depos.* **2024**, *18*, 9–17. [CrossRef]
10. Jia, T.; Guo, T.; Yao, Y.; Wang, R.; Chai, B. Seasonal Microbial Community Characteristic and Its Driving Factors in a Copper Tailings Dam in the Chinese Loess Plateau. *Front. Microbiol.* **2020**, *11*, 1574. [CrossRef]
11. Hao, R.; Li, D.; Zhang, J.; Jiao, T. Green Synthesis of Iron Nanoparticles Using Green Tea and Its Removal of Hexavalent Chromium. *Nanomaterials* **2021**, *11*, 650. [CrossRef]
12. Abdykadyrov, A.; Abdullayev, S.; Tashtay, Y.; Zhunussov, K.; Marxuly, S. Purification of surface water by using the corona discharge method. *Min. Miner. Depos.* **2024**, *18*, 125–137. [CrossRef]
13. Kuang, X.; Wang, W.; Hu, J.; Liu, W.; Zeng, W. Subcellular distribution and chemical forms of manganese in Daucus carota in relation to its tolerance. *Front. Plant Sci.* **2022**, *13*, 947882. [CrossRef]
14. Long, J.; Tan, D.; Deng, S.; Lei, M. Pollution and ecological risk assessment of antimony and other heavy metals in soils from the world's largest antimony mine area, China. *Hum. Ecol. Risk Assess. Int. J.* **2017**, *24*, 679–690. [CrossRef]
15. Li, H.; Liu, Q. Reaction medium for permeable reactive barrier remediation of groundwater polluted by heavy metals. *Front. Environ. Sci.* **2022**, *10*, 968546. [CrossRef]
16. Chen, X.; Li, F.; Zhang, J.; Liu, S.; Ou, C.; Yan, J.; Sun, T. Status, fuzzy integrated risk assessment, and hierarchical risk management of soil heavy metals across China: A systematic review. *Sci. Total Environ.* **2021**, *785*, 147180. [CrossRef] [PubMed]
17. Mohd Pu'ad, N.A.S.; Abdul Haq, R.H.; Mohd Noh, H.; Abdullah, H.Z.; Idris, M.I.; Lee, T.C. Synthesis method of hydroxyapatite: A review. *Mater. Today Proc.* **2020**, *29*, 233–239. [CrossRef]
18. Song, Y.; Zhang, M.; Li, H.; Yang, Y.; Chen, X.; Li, J.; Brogi, A. Effect of Chromium Ion on the Strength Characteristics and Damage Law of Red Clay. *Geofluids* **2022**, *2022*, 8451476. [CrossRef]
19. Kong, L.; Liu, X.; Lv, G.; Liu, T.; Zhang, P.; Li, Y.; Chen, B.; Liao, L.; Zhang, T. Copper Adsorption Using Hydroxyapatite Derived from Bovine Bone. *Adv. Civ. Eng.* **2022**, *2022*, 1026129. [CrossRef]
20. Fuller, C.C.; Bargar, J.R.; Davis, J.A. Molecular-Scale Characterization ofUranium Sorption by Bone ApatiteMaterials for a Permeable ReactiveBarrier Demonstration. *Environ. Sci. Technol.* **2003**, *37*, 4642–4649.
21. Adhikari, T.; Dharmarajan, R.; Lamb, D.; Zhang, H. Remediation of Frogmore Mine Spoiled Soil with Nano Enhanced Materials. *Soil Sediment Contam. Int. J.* **2021**, *31*, 367–385. [CrossRef]
22. Chen, M.; Zhang, Z.; Hu, X.; Tian, J.; Wang, J.; Wan, R.; Cui, X.; Zhou, X.; Liu, D. Adsorption of $Si(OH)_4$ and $Al(OH)_4$ onto arsenopyrite surface: Exploring the sealing feasibility of geopolymer to arsenopyrite. *Miner. Eng.* **2021**, *170*, 107017. [CrossRef]
23. Huang, X.; Zhu, F.; He, Z.; Chen, X.; Wang, G.; Liu, M.; Xu, H. Photosynthesis Performance and Antioxidative Enzymes Response of *Melia azedarach* and *Ligustrum lucidum* Plants Under Pb–Zn Mine Tailing Conditions. *Front. Plant Sci.* **2020**, *11*, 571157. [CrossRef]
24. Wang, P.; Sun, Z.; Hu, Y.; Cheng, H. Leaching of heavy metals from abandoned mine tailings brought by precipitation and the associated environmental impact. *Sci. Total Environ.* **2019**, *695*, 133893. [CrossRef]
25. Yu, Q.; Liu, H.; Lv, G.; Liu, X.; Wang, L.; Liao, L. Mechanistic insight into lead immobilization on bone-derived carbon/hydroxyapatite composite at low and high initial lead concentration. *Sci. Total Environ.* **2023**, *900*, 165910. [CrossRef]
26. Joshi, P.; Manocha, S. Kinetic and thermodynamic studies of the adsorption of copper ions on hydroxyapatite nanoparticles. *Mater. Today Proc.* **2017**, *4*, 10455–10459. [CrossRef]
27. Sellaoui, L.; Mendoza-Castillo, D.I.; Reynel-Ávila, H.E.; Bonilla-Petriciolet, A.; Ben Lamine, A.; Erto, A. A new statistical physics model for the ternary adsorption of Cu^{2+}, Cd^{2+} and Zn^{2+} ions on bone char: Experimental investigation and simulations. *Chem. Eng. J.* **2018**, *343*, 544–553. [CrossRef]

28. Ben-Ali, S.; Jaouali, I.; Souissi-Najar, S.; Ouederni, A. Characterization and adsorption capacity of raw pomegranate peel biosorbent for copper removal. *J. Clean. Prod.* **2017**, *142*, 3809–3821. [CrossRef]
29. Kali, A.; Amar, A.; Loulidi, I.; Jabri, M.; Hadey, C.; Lgaz, H.; Alrashdi, A.A.; Boukhlifi, F. Characterization and adsorption capacity of four low-cost adsorbents based on coconut, almond, walnut, and peanut shells for copper removal. *Biomass Convers. Biorefinery* **2022**, *14*, 3655–3666. [CrossRef]
30. Xue, Y.; Yu, Q.; Fang, J.; Jia, Y.; Wang, R.; Fan, J. A Wetting and Capture Strategy Overcoming Electrostatic Repulsion for Electroreduction of Nitrate to Ammonia from Low-Concentration Sewage. *Small* **2024**, *20*, 2400505. [CrossRef]
31. Xue, Y.; Yu, Q.; Ma, Q.; Chen, Y.; Zhang, C.; Teng, W.; Fan, J.; Zhang, W.-x. Electrocatalytic Hydrogenation Boosts Reduction of Nitrate to Ammonia over Single-Atom Cu with Cu(I)-N3C1 Sites. *Environ. Sci. Technol.* **2022**, *56*, 14797–14807. [CrossRef]
32. Kızıltas Demir, S.; Tugrul, N. Zinc and cadmium adsorption from wastewater using hydroxyapatite synthesized from flue gas desulfurization waste. *Water Sci. Technol.* **2021**, *84*, 1280–1292. [CrossRef]
33. Zhu, Z.; Wu, Y.; Hu, C.; Zhang, L.; Ding, H.; Zhu, Y.; Fan, Y.; Deng, H.; Zhou, X.; Tang, S. Elimination of zinc ions from aqueous solution by a hydroxylapatite-biochar composite material with the hierarchical porous microstructures of sugarcane waste. *J. Clean. Prod.* **2022**, *362*, 132483. [CrossRef]
34. Rudi, N.N.; Muhamad, M.S.; Te Chuan, L.; Alipal, J.; Omar, S.; Hamidon, N.; Abdul Hamid, N.H.; Mohamed Sunar, N.; Ali, R.; Harun, H. Evolution of adsorption process for manganese removal in water via agricultural waste adsorbents. *Heliyon* **2020**, *6*, e05049. [CrossRef]

Disclaimer/Publisher's Note: The statements, opinions and data contained in all publications are solely those of the individual author(s) and contributor(s) and not of MDPI and/or the editor(s). MDPI and/or the editor(s) disclaim responsibility for any injury to people or property resulting from any ideas, methods, instructions or products referred to in the content.